microbial biotechnology

Open Access

Increasing the copper sensitivity of microorganisms by restricting iron supply, a strategy for bio-management practices

Anne Soisig Steunou,* Marie-Line Bourbon, Marion Babot, Anne Durand, Sylviane Liotenberg, Yoshiharu Yamaichi and Soufian Ouchane**

Institute for Integrative Biology of the Cell (I2BC), CEA, CNRS, Université Paris-Saclay, 91198, Gif-sur-Yvette, France.

Summary

Pollution by copper (Cu^{2+}) extensively used as antimicrobial in agriculture and farming represents a threat to the environment and human health. Finding ways to make microorganisms sensitive to lower metal concentrations could help decreasing the use of Cu^{2+} in agriculture. In this respect, we showed that limiting iron (Fe) uptake makes bacteria much more susceptible to Cu^{2+} or Cd^{2+} poisoning. Using efflux mutants of the purple bacterium *Rubrivivax gelatinosus,* we showed that Cu^{+} and Cd^{2+} resistance relies on the expression of the Fur-regulated FbpABC and Ftr iron transporters. To support this conclusion, inactivation of these Fe-importers in the Cu^{+} or Cd^{2+}-ATPase efflux mutants gave rise to hypersensitivity towards these ions. Moreover, in metal overloaded cells the expression of FbpA, the periplasmic iron-binding component of the ferric ion transport FbpABC system was induced, suggesting that cells perceived an 'iron-starvation' situation and responded to it by inducing Fe-importers. In this context, the Fe-Sod activity increased in response to Fe homoeostasis dysregulation. Similar results were obtained for *Vibrio cholerae* and *Escherichia coli,* suggesting that perturbation of Fe homoeostasis by metal excess appeared as an adaptive response commonly used by a variety of bacteria. The presented data support a model in which metal excess induces Fe-uptake to support [4Fe-4S] synthesis and thereby induce ROS detoxification system.

Received 27 January, 2020; revised 15 April, 2020; accepted 16 April, 2020.
For correspondence. *E-mail anne.soisig.steunou@i2bc.paris-saclay.fr; Tel. +(33)-169823137; Fax +(33)-169823230. **E-mail soufian.ouchane@i2bc.paris-saclay.fr; Tel. +(33)-169823137; Fax +(33)-169823230.
Microbial Biotechnology (2020) **13**(5), 1530–1545
doi:10.1111/1751-7915.13590
Funding information
We gratefully acknowledge the support of the CNRS and the Microbiology Department of I2BC.

Introduction

Although copper serves as a catalytic cofactor to drive a variety of biochemical processes including respiration and photosynthesis (Andreini *et al.*, 2008), excess Cu^{2+}, exceeding cellular needs, is toxic. Copper is thus the main toxic component in the 'Bordeaux Mixture', an effective bactericide and fungicide used for decades in agriculture to control diseases of vine fruits, olive groves, ornamental plants and fruit orchards. The extensive use of Cu^{2+} as a fungicide against mildew in vineyards or in farming, for example, is a source of soils and groundwater contamination. Furthermore, extensive use of metals at high concentrations appears to promote co-occurrence and co-selection of antibiotic resistance genes with metal resistance gene (Baker-Austin *et al.*, 2006; Rensing *et al.*, 2018; Asante and Osei Sekyere, 2019).

A recent study reported the factors influencing copper distribution in agricultural lands at the European scale and highlighted the importance of land management practices in copper concentration and the strong correlation between topsoil copper and vineyards. (Ballabio *et al.*, 2018). Moreover, the increased copper concentration in soil over a long period was shown to negatively affect bacterial richness and evenness (Nunes *et al.*, 2016). The European Commission also pinpointed the environmental and health risk associated with high copper concentration use in agriculture and the urgent need for more sustainable 'metal-based antimicrobial treatments' management to limit the spread of copper and its adverse effects on ecosystems and living organisms.

https://ec.europa.eu/environment/integration/research/newsalert/pdf/agricultural_management_practices_influence_copper_concentrations_european_topsoils_518_na2_en.pdf

Both prokaryotes and eukaryotes deal with metals such as Cu^{+}, Zn^{2+} or Fe^{2+} and maintain optimal cytoplasmic concentration either by storing the excess using specific proteins and compartments or by blocking the import using regulators to repress gene expression or expelling the excess using the efflux systems. Copper balance in bacteria relies mainly on efflux systems. When the homoeostasis system is dysregulated,

accumulation of Cu^+ could directly lead, through Fenton-like chemistry, to hydroxyl radical generation (Gunther *et al*., 1995). Cu^+ can also displace iron from proteins or damage exposed [4Fe-4S] clusters resulting in released Fe atoms (Macomber and Imlay, 2009; Barwinska-Sendra and Waldron, 2017) that can induce iron-based Fenton chemistry and reactive oxygen species (ROS) production. As with Cu^+, Cd^{2+}, a non-biological and non-redox active metal, can also trigger iron-based Fenton chemistry. This supports the idea that excess Cd^{2+} could give rise to intracellular mismetallation of proteins and release of 'free iron' (Xu and Imlay, 2012). One may expect that under such conditions, cells will repress iron uptake to limit the harmful effects of excess iron and ROS. Inconsistently, however, several transcriptomic studies in bacteria, yeast or plants reported that excess Cu^+, Cd^{2+}or Co^+ induced iron uptake gene expression (Gross *et al*., 2000; Stadler and Schweyen, 2002; Teitzel *et al*., 2006; Yoshihara *et al*., 2006; Houot *et al*., 2007; Chillappagari *et al*., 2010). In *Escherichia (E.) coli,* expression of some genes involved in the synthesis and uptake of siderophore or iron was induced when cells were exposed to excess Cu^+, Zn^{2+}, Ni^{2+} or Co^{2+} (Kershaw *et al*., 2005; Fantino *et al*., 2010; Macomber and Hausinger, 2011; Xu *et al*., 2019). Similarly, in *Pseudomonas (P.) aeruginosa*, several genes involved in iron uptake, usually induced under iron-limiting condition, were also upregulated in Cu^+ stressed cells (Teitzel *et al*., 2006). Interestingly, in *Bacillus subtilis*, microarray data indicated that Cu^+ stress-induced genes were required for iron uptake, whereas induction of the Cu^+ efflux system CopZA in the Δ*csoR* Cu^+-sensing transcriptional repressor mutant prevented upregulation of these Fur-regulated genes (Chillappagari *et al*., 2010).

In the yeast *Saccharomyces cerevisiae*, it was also shown that elevated amount of Cu^+ or Co^+ induced the expression of the iron regulon (Fet, Ftr), thereby increasing the intracellular iron level (Gross *et al*., 2000; Stadler and Schweyen, 2002; Alkim *et al*., 2013). On the other hand, Cd^{2+} was shown to upregulate the genes involved in Fe acquisition, in the cyanobacterium *Synechocystis PCC6803*, in the green alga *Chlamydomonas reinhardtii* or in plants (Rubinelli *et al*., 2002; Yoshihara *et al*., 2006; Houot *et al*., 2007) but not in *E. coli* (Helbig *et al*., 2008). In agreement with these reports, it was shown that co-incubation of Cu^+ stressed hepatocytes with the iron chelator deferoxamine significantly inhibited ROS production and prevented cell death. This suggested an increased iron uptake under Cu^+ excess stress in hepatocytes (Krumschnabel *et al*., 2005). Although these studies provided indirect evidence for a central role of iron homoeostasis to cope with excess metal, an understanding of the underlying processes at a molecular level is still lacking.

In the context of metal stress, exposure of the efflux mutants Δ*copA* (the Cu^+-efflux ATPase) or Δ*cadA* (the Zn^{2+}/Cd^{2+} efflux ATPase) to elevated Cu^+ or Cd^{2+} level resulted in coproporphyrin III accumulation in the purple non-sulphur photosynthetic bacterium *Rubrivivax (R.) gelatinosus* (Azzouzi *et al*., 2013; Steunou *et al*., 2020a) and in *Neisseria gonorrhea* (Djoko and McEwan, 2013), likely denoting an effect on [4Fe-4S] clusters. *R. gelatinosus* can grow either by respiration or by photosynthesis and tolerate high concentration of Cu^{2+} and Cd^{2+} (Azzouzi *et al*., 2013; Steunou *et al*., 2020a). To better decipher the consequences of excess Cu^+ or Cd^{2+} in *R. gelatinosus,* we used transposon mutagenesis to select and characterize hypersensitive mutants to Cu^+ and to Cd^{2+}. Unexpectedly, most isolated mutations were found within the *fbpA* gene, encoding the periplasmic iron-binding protein (FbpA) component of the ferric iron FbpABC system. It is interesting that both Cu^+ and Cd^{2+} elicited similar phenotypes, that is [4Fe-4S] degradation in *E. coli* or in *R. gelatinosus*. This provided opportunity to address the impact of redox-active and non-active metals on iron homoeostasis in bacteria, with a focus on the events that followed [4Fe-4S] clusters degradation after Cu^+ or Cd^{2+} stress. Based on previous work from various groups, our study allowed us to draw a model on how excess Cu^+ or Cd^{2+} would poison cells, starting with protein mismetallation to ROS generation. The central role of Fe-uptake, likely to maintain Fe-S clusters synthesis, in response to Cu^+ or Cd^{2+} homoeostasis dysregulation in bacteria and eukaryotes is also discussed. Metal-based antimicrobial strategies using copper or cadmium have potential applications in many fields; nevertheless, sustainable practices to avoid metal pollution must be found (Turner, 2017). Here, we demonstrated that limiting iron uptake is an effective way to inhibit bacterial growth with very low copper concentration.

Results

Iron uptake provided a survival advantage during copper or cadmium stress

A genetic approach using Tn5 random mutagenesis system in *R. gelatinosus* was applied to select mutants with increased sensitivity to Cu^+ and Cd^{2+} in the double mutant Δ*copRcadR* background, in which both metal regulators CopR and CadR were inactivated. CopR activates the expression of *cop* operon in response to excess Cu^+, and CadR activates *cadA* expression in presence of Cd^{2+} (Azzouzi *et al*., 2013; Steunou *et al*., 2020a). Under photosynthesis condition, this mutant can still grow in presence of 400 μM $CuSO_4$ and $CdCl_2$, because the Cu^+-exporting ATPase CopA and the Cd^{2+} efflux pump CadA are still expressed, albeit at lower level. Upon screening for transposon mutants unable to

survive on 50 μM $CuSO_4$, 5 out of 10 hypersensitive Δ*copRcadR::Tn* mutants had the transposon inserted within the *fbpA* gene at different positions (Fig. S1). These mutants were also sensitive to 50 μM $CdCl_2$. Strikingly, *fbpA* gene is predicted to play a role in iron uptake. *fbpA* encodes the periplasmic substrate-binding protein component of the membrane ABC-type iron (Fe^{3+}) transporter, FbpABC (Fig. S2; Parker Siburt *et al*., 2012). Unlike many other bacteria, *R. gelatinosus fbpA* and *fbpBC* genes are not organized in a single operon but split in the genome. Nonetheless, putative *Fur* boxes were identified in the promoter of *fbpA* and *fbpBC* genes suggesting that this system could be induced under iron limitation (Fig. S1). All of the five Δ*copRcadR-fbpA::Tn* mutants exhibited comparable growth in medium containing increased concentrations of $CuSO_4$ or $CdCl_2$ (Fig. S1).

Dose–response growth experiments confirmed that, in contrast to the parental Δ*copRcadR* strain, the transposon triple mutant Δ*copRcadR-fbpA::Tn* was more sensitive to copper and cadmium (Fig. 1A and B). Hereafter, we used Δ*copRcadR-fbpA2*::Tn5 insertion mutant, in which Tn5 was found at position 477 in the *fbpA* gene, for further investigation. These data suggested that FbpA plays an important role in the tolerance mechanisms towards Cu^+ and Cd^{2+}.

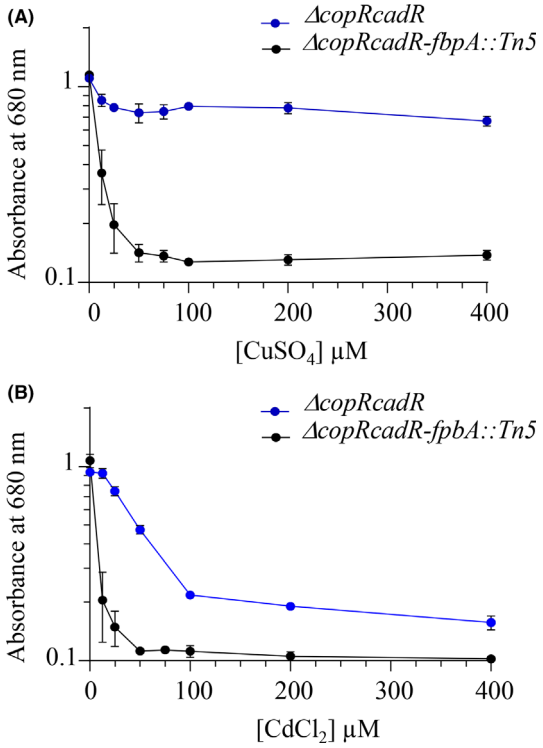

Fig. 1. FbpA is involved in copper and cadmium tolerance. Growth inhibition of the Δ*copRcadR* and Δ*copRcadR-fpbA2::Tn5* mutant in malate medium supplemented with increasing $CuSO_4$ (A) or $CdCl_2$ (B) concentrations under photosynthesis condition. Cells were inoculated with an OD_{680} of 0.02 and grown overnight for 18 h at 30°C before OD_{680nm} measurement. Results are the average of 3 independent experiments.

Hypersusceptibility of the ATPase-deficient mutants upon inactivation of the periplasmic iron-binding protein FbpA

To confirm the transposon mutant phenotype, *fbpA2::Tn5* allele was transferred in the wild-type, in the Cu^+-ATPase (*copATp)* or in the Cd^{2+}-ATPase (Δ*cadATp)* deficient mutants. Their sensitivity to Cu^+ or Cd^{2+} under photosynthesis condition was examined. In contrast to the wild-type and the *fbpAKm* mutant that can tolerate up to 400 μM $CuSO_4$ in the medium, growth of the *copATp* mutant was affected by increasing concentration of $CuSO_4$ and inhibited beyond 200 μM $CuSO_4$ (Table S1). Inactivation of the *fbpA* gene in the *copATp* background led to a hypersensitive strain. Indeed, growth was drastically decreased even in malate medium that contained only 1.6 μM $CuSO_4$ and was completely inhibited when the medium was supplemented with 50 μM $CuSO_4$ (Fig. 2A). This Cu^+-sensitive phenotype was even more pronounced than the phenotype observed for Δ*copRcadR-fbpA::Tn* mutant, likely because the latter still expressed CopA and expelled some Cu^+ outside the cytoplasm. Similarly, the Δ*cadAfbpA* mutant was more sensitive to Cd^{2+} than the single Δ*cadATp* and *fbpAKm* mutants, confirming that *fbpA* was somehow also involved in Cd^{2+} tolerance (Fig. 2B). Altogether, these data indicated that *fbpA* expression and presumably iron uptake were required for Cu^+ and Cd^{2+} tolerance in the absence of the detoxification efflux systems.

Hypersusceptibility to Cu^+ is associated with increased coproporphyrin III production in the absence of FbpA

Toxicity of copper in the ATPase-deficient mutant *copA*$^-$ of *R. gelatinosus* and *Neisseria gonorrhea* was related to an impaired porphyrin biosynthesis illustrated by the release of coproporphyrin III (oxidized coproporphyrinogen III) in the medium. Under this condition, excess copper is likely to damage the iron–sulphur cluster of the coproporphyrinogen III oxidase HemN (Azzouzi *et al*., 2013; Djoko and McEwan, 2013). Combination of severe decrease of porphyrins/increased release of coproporphyrin III and impaired iron uptake might explain the Cu^+ sensitivity phenotype of *copAfbpA*$^-$ strain. To establish a correlation between Cu^+ concentration, coproporphyrin III release and *fbpA* gene disruption, the growth of wild-type, *copATp, fbpAKm* and *copAfbpA*$^-$ cells was challenged with very low $CuSO_4$ concentration ranging from 2 to 6 μM. As discussed above, the growth of *copAfbpA*$^-$ mutant was affected even at very low concentration of $CuSO_4$. Under these conditions, concentration of coproporphyrin

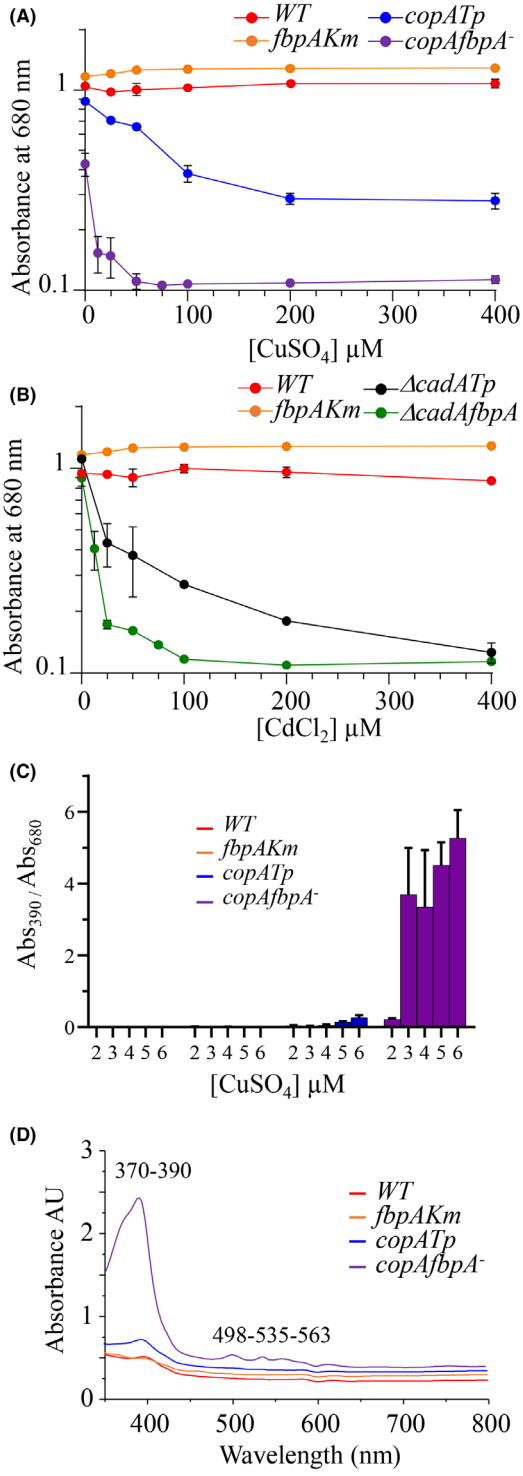

Fig. 2. FbpA is required for copper and cadmium tolerance when the efflux systems are defective. Growth inhibition of the *copAfbpA*$^{-}$ (A), Δ*cadAfbpA* (B) in comparison with the wild-type and the single mutants in malate medium supplemented with increasing $CuSO_4$ or $CdCl_2$ concentration under photosynthesis condition. Cells were grown overnight for 18 h at 30°C before OD_{680nm} measurement. Results are the average of 3 independent experiments. C. Quantification of coproporphyrin III in the medium was performed by absorbance (maxima at 390 nm), and values were normalized with the absorbance of the culture at 680 nm. The mean and standard deviation of four independent experiments were shown. D. Absorbance spectra of the spent medium of wild-type and mutant strains. Representative spectra curves of four independent experiments are shown.

III released in the culture supernatant was spectroscopically analysed. As shown in Fig. 2C and D, no coproporphyrin III could be detected in the medium of wild-type or *fbpAKm* mutant cells regardless of the copper concentration. In the *copATp* cells, coproporphyrin III could only be detected in the medium containing at least 5 µM $CuSO_4$. Noticeably, for the *copAfbpA*$^{-}$ mutant, higher amount of coproporphyrin III was detected even in the growth medium containing only 2 µM $CuSO^4$. The amount of released coproporphyrin III was significantly increased in the medium containing 3 µM $CuSO_4$ (Fig. 2C and D). These data showed that the effect of copper on porphyrin biosynthesis was more pronounced when both the ATPase CopA and the iron uptake system Fbp were inactivated.

Excess Cu^+ or Cd^{2+} induces the expression of the periplasmic iron-binding protein FbpA

Previous transcriptomic studies in bacteria have suggested an induction of different iron uptake systems in response to excess copper (Kershaw *et al.*, 2005; Teitzel *et al.*, 2006; Chillappagari *et al.*, 2010). Our genetics data strongly suggest the expression of the iron uptake FbpABC system in *R. gelatinosus* under Cu^+ or Cd^{2+} excess stress. Moreover, semi-quantitative RT-qPCR showed a ~2-fold induction of *fbpA* transcripts in response to iron starvation and to Cu^+ or Cd^{2+} excess (Fig. S3). In order to follow FbpA protein expression under different metallic stress conditions, the *fbpA* gene was substituted by a histidine-tagged copy (*fbpAH*$_6$) on the chromosome under its own Fur-regulated promoter. This strain was subjected to elevated concentration of $CuSO_4$ or $CdCl_2$ either in an iron-containing or in iron-limited medium and the amount of $FbpAH_6$ in the periplasmic fraction was assessed on Western blots (Fig. 3). In the iron-containing medium with basal 1.6 µM $CuSO_4$, $FbpAH_6$ was not detected. On the contrary, in the medium supplemented with 250 or 500 µM $CuSO_4$ a gradual increase in the amount of $FbpAH_6$ was observed in the periplasm. This increase correlated with the gradual increase in the amount of CopI, the periplasmic Cu^+-induced protein (Fig. 3A), which can be also detected by the HisProbe due to its histidine-rich motif (Durand *et al.*, 2015). Under iron-limited condition,

$FbpAH_6$ was detected in the periplasmic fraction even in the malate medium containing 1.6 μM $CuSO_4$. This expression was very likely related to iron limitation in the medium. As expected, addition of 250 or 500 μM $CuSO_4$ to this medium resulted in a substantial induction of $FbpAH_6$ and CopI. Similar induction of $FbpAH_6$ and CopI was obtained with addition of high concentrations of $CdCl_2$ to the growth medium (Fig. 3B), confirming the induction of FbpA when excess Cd^{2+} was present in the medium.

These data argued in favour of an induction of the iron transporter FbpA by excess Cu^{+} or Cd^{2+}, and interestingly, FbpA induction underlied an iron 'depletion-like' situation in cells facing excess metal. To test this assumption, we also investigated the effect of excess Cu^{+} or Cd^{2+} stress on total iron content in cells grown in medium supplemented or not with excess metal. ICP-MS analyses showed a decrease in the amount of total iron content in the *copATp* cells challenged with 100 μM $CuSO_4$ and Δ*cadATp* cells challenged with 100 μM $CdCl_2$ (Fig. 3C). In the wild-type, the amount of total iron remained comparable under both stress conditions confirming that Cu^{+} or Cd^{2+} excess altered Fe^{2+} homoeostasis in the efflux mutant that accumulated metals within the cytoplasm.

Hypersusceptibility of the ATPase-deficient mutants upon disruption of the iron uptake system fbpBC

fbpABC is proposed to encode a periplasmic binding protein-dependent ABC transport system that enables iron transport in Gram- bacteria. The *fbpBC* genes encode the cytoplasmic membrane-associated proteins FbpB and FbpC that act together with FbpA for the transport of

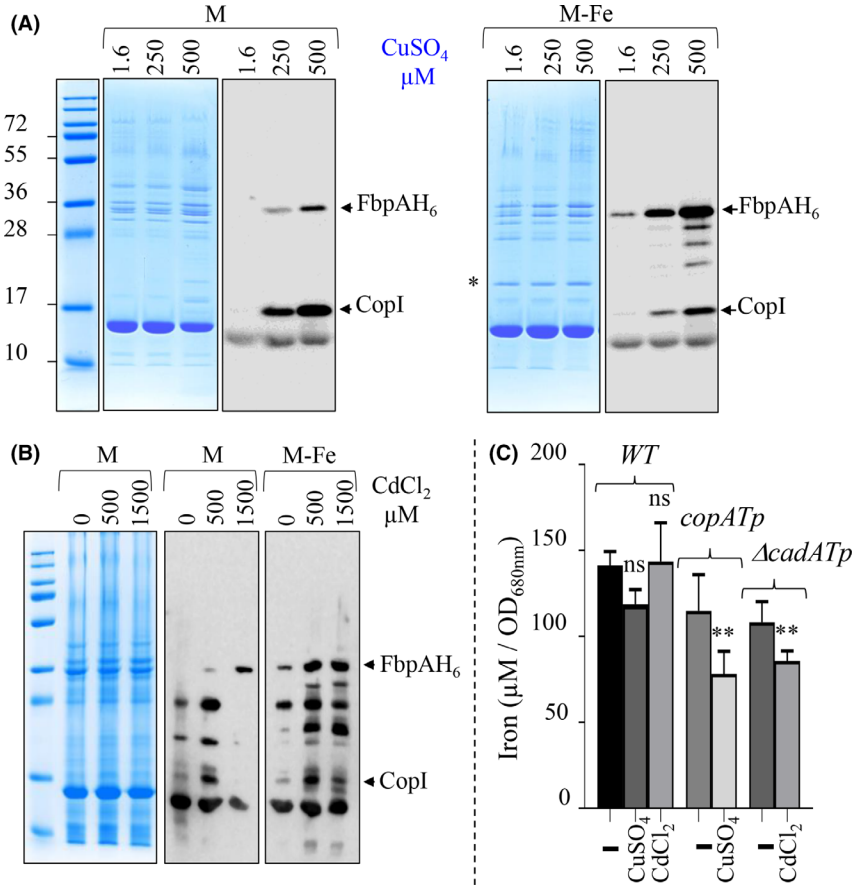

Fig. 3. Expression of the periplasmic iron-binding protein FbpA is induced under excess copper and cadmium or under iron limitation. *fbp*AHis$_6$ cells were grown overnight for 18 h in the presence of increasing concentration of $CuSO_4$ (A) or $CdCl_2$ (B), in malate medium (M) or iron-depleted malate medium (M-Fe). The presence of $FbpAH_6$ and CopI was revealed in the periplasmic fractions using the HRP-HisProbe. CopI is induced by copper and cadmium and served as an internal control. * 19 kDa protein induced in iron-depleted medium. C. Cu^{+} or Cd^{2+} excess affects the intracellular iron content in the ATPase efflux mutants. Intracellular content of iron in the *WT, copATp and ΔcadATp* was measured by ICP-MS. The values were normalized by the culture absorbance at 680 nm. The results are expressed as the mean ± SD (error bars). Significance of variation between wild-type in malate medium and samples were determined by one-way ANOVA with Dunnett's multiple comparison test. ns, non-significant; $^{**}P < 0.01$.

iron into the cell. Although the involvement of FbpA as a periplasmic binding protein in the Cu^{+} or Cd^{2+} response and resistance is now well established, the involvement of FbpBC proteins in Cu^{+} or Cd^{2+} response remains to be demonstrated to unequivocally state that the FbpABC iron transport system is involved in metal excess tolerance. To this aim, the *fbpBC* locus was deleted in the wild-type and efflux mutants, *copAKm* and Δ*cadAKm* strains. The tolerance of the double mutant towards Cu^{+} or Cd^{2+} excess was assessed and compared to that of the wild-type and the single mutants (Fig. 4). As expected, while the wild-type and the Δ*fbpBC* mutant tolerated up to 400 μM $CuSO_4$ in the medium, growth of the *copAKm* mutant was affected by increasing concentration of $CuSO_4$ and inhibited at 200 μM $CuSO_4$ (Fig. 4B and C). Deletion of the *fbpBC* genes in the *copAKm* background gave a hypersensitive Δ*copAfbpBC* strain, in which growth was dramatically decreased by excess Cu^{+} and completely inhibited in medium containing 50 μM $CuSO_4$ (Fig. 4B and C). This Cu^{+}-sensitive phenotype was comparable to that observed for the *copAfbpA*$^{-}$ mutant demonstrating that, as for FbpA, the membrane cytoplasmic FbpBC transporter, which uses ATP hydrolysis to drive iron transport into the cytoplasm, was also required for copper tolerance when the Cu^{+}-efflux system was missing. Similarly, the Δ*cadAfbpBC* mutant was more sensitive to Cd^{2+} than the single mutants (Fig. 4D), confirming that *fbpBC* was also involved in Cd^{2+} tolerance.

Altogether, these data strongly indicated that the iron acquisition FbpA/FbpBC system and very likely iron uptake were required for Cu^{+} and Cd^{2+} tolerance in the absence of the efflux detoxification systems.

The Ftr iron import system is also required for metal tolerance

The *fbpAKm* and Δ*fbpBC* mutants still grew in the malate medium with excess Cu^{+} or Cd^{2+} suggesting the presence of other iron uptake systems. To analyse the *R. gelatinosus* response to iron limitation, the wild-type and *fbpAKm* strains were cultured in parallel either in iron-containing or in iron-depleted media and periplasmic fractions were analysed on SDS-PAGE. This analysis revealed a strong induction of a 19 kDa protein (Figs 3A and 5A). The search for periplasmic protein-encoding genes within the *R. gelatinosus* genome database suggested that this protein might correspond to FtrA (also annotated as P19), involved in Fe^{3+} uptake. To ascertain that the induced protein under iron-limiting condition corresponded to FtrA, the *ftrA* gene was inactivated in the wild-type strain and the periplasmic protein content was compared under iron-rich and iron-depleted condition. The analysis confirmed that the identified band corresponded to FtrA as it was absent in the Δ*ftrATp* strain (Fig. 5A). FtrA/P19 is the periplasmic iron-binding protein of the tripartite FtrABC (EfeUOB) and P19-Ftr1P system identified in *Escherichia coli* strain O157:H7 and *Campylobacter jejuni* respectively (Cao *et al*., 2007; Liu *et al*., 2018). FtrA encoding gene in *R. gelatinosus* was found within a putative Fur-regulated operon of five genes, *ftrAPBCD,* also encoding an outer membrane protein (FtrP), a putative periplasmic Cu-oxidase protein (FtrB), a permease (FtrC) and a membrane polyferredoxin (FtrD) (Fig. S2). To assess whether this iron uptake system was required for excess metal resistance in *R. gelatinosus*, the *ftrA* gene was also inactivated in *copAKm* and Δ*cadAKm* mutant. Analyses of growth inhibition in the Δ*copAftrA or* Δ*cadAftrA* mutants showed that these mutants were more sensitive to excess metal than the single mutants *copA*$^{-}$ (Fig. 5B) and Δ*cadA* (Fig. 5C) and revealed that, as FbpA, FtrA was also involved in the tolerance to excess Cu^{+} or Cd^{2+}. Semi-quantitative RT-PCR also confirmed the induction of *ftrA* under iron-depleted condition and under excess Cu^{+} or Cd^{2+} (Fig. S3).

Given the evidence that both iron uptake systems Fbp and Ftr contributed to the Cu^{+} and Cd^{2+} resistance, we anticipated that inactivation of the two iron uptake systems may display increased sensitivity to excess Cu^{+} or Cd^{2+}. We therefore generated a double mutant Δ*ftrAfbpA* and analysed its ability to grow in the presence of excess Cu^{+} or Cd^{2+}. The Δ*ftrAfbpA* growth was not affected in malate medium, probably thanks to the presence of other iron transporters like FeoAB. Nonetheless, growth of the Δ*ftrAfbpA* mutant was more affected under iron-depleted condition suggesting that FeoAB is not sufficient under iron-limiting condition. As shown in Figure 5D and E, the Δ*ftrATp* or *fbpAKm* single mutants behave as the wild-type and tolerate metal excess in the medium. In sharp contrast, the Δ*ftrAfbpA* double mutant displayed sensitivity to both Cu^{+} and Cd^{2+}. Taken together, these data indicated that iron import through Fbp and Ftr systems (Fig. S2) was required to face excess Cu^{+} or Cd^{2+} in the cytoplasm.

Iron import is also required for Cu^{+} tolerance in Vibrio cholerae

Vibrio cholerae, an aquatic bacterium that can infect human intestine to cause diarrhoeal diseases, has a copper efflux system comparable to that of *R. gelatinosus*. Both include the Cu^{+}-ATPase CopA and the periplasmic CopI protein induced by excess copper, while lacking the Cus system. Taking into account the results presented here for *R. gelatinosus*, we assumed that inactivation of the iron transporter FbpA in a *copA*-

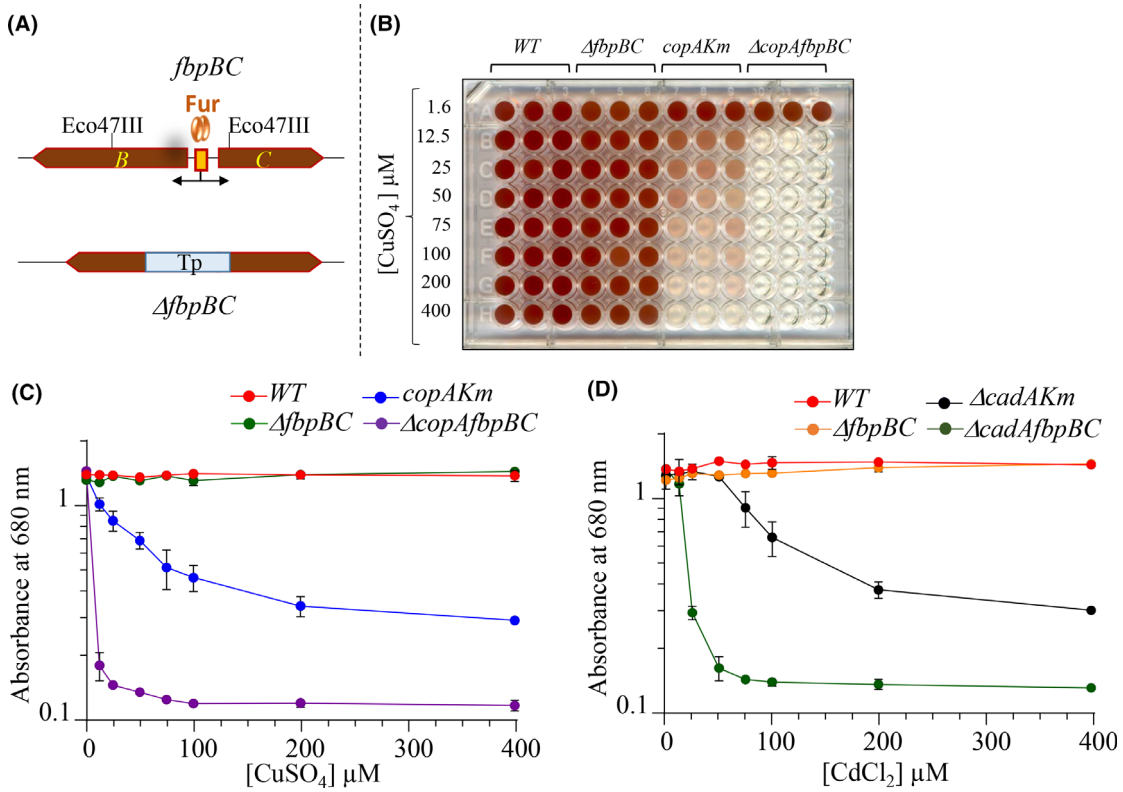

Fig. 4. The iron importer FbpBC is required for copper and cadmium tolerance when the efflux system is defective. Organization and deletion of *fbpBC* genes. A trimethoprim cassette was inserted in the Eco47III restriction enzyme sites deleting *fbpB* and *fbpC* genes (A). Growth of the WT, Δ*fbpBC, copAKm* and the double mutant Δ*copAfbpBC* cells under photosynthesis in presence of increasing $CuSO_4$ concentrations after 18 h (B). Growth inhibition curves of the Δ*copAfbpBC* (C), Δ*cadAfbpBC* (D) in comparison with the *WT* and the single mutants in malate medium supplemented with increasing $CuSO_4$ or $CdCl_2$ concentrations under photosynthesis condition. Cells were inoculated at 0.02 and grown overnight for 18 h at 30°C before OD_{680nm} measurement. Results are the average of 3 independent experiments.

deficient background would lead to a hypersensitive strain to excess copper in *V. cholerae* as well. To test this assumption, the effect of $CuSO_4$ on the growth in liquid LB medium of the Δ*copAfbpA* disruption strain was compared with the Δ*fbpA,* Δ*copA* and wild-type strains (Fig. 6). As expected, the Δ*copA* strain exhibited decreased resistance to $CuSO_4$. Yet, growth inhibition by $CuSO_4$ was more pronounced in the double mutant Δ*copAfbpA,* confirming the role of iron in Cu^+ tolerance in this bacterium. We should stress out that in contrast to *R. gelatinosus*, *V. cholerae* possesses a wide battery of iron transport systems that could help the bacterium to face excess copper in order to occupy different niches (Payne *et al*., 2016).

Under Cu^+ excess stress, Fe-Sod activity correlates with an iron dysregulation status in E. coli, but not in R. gelatinosus and V. cholerae

It is well established that the expression of superoxide dismutases (SOD), Mn-Sod SodA and Fe-Sod SodB is regulated by iron status in bacteria. This regulation involves the Fur repressor and in some species the sRNA RyhB that downregulate nonessential iron-containing proteins when iron is limited (Masse and Gottesman, 2002; Troxell and Hassan, 2013; Imlay, 2019). In *E. coli*, under iron-limiting condition, the Fe-Sod expression was repressed, whereas the Mn-Sod was induced to convert superoxide into H_2O_2 and protect the cell from oxidative stress (Carlioz and Touati, 1986). Fe-Sod and Mn-Sod activities could thus reflect the iron status within the cells. Our results, showing that excess Cu^+ induced the induction of iron transporter and likely elicited iron limitation, prompted us to check the activity and expression of the superoxide dismutases in *R. gelatinosus, V. cholerae* and *E. coli* in response to excess Cu^+.

In contrast to *E. coli,* in which both the Fe-Sod and Mn-Sod are active, *R. gelatinosus* genome encodes only the cytosolic Fe-Sod superoxide dismutase. To understand how the bacterium controls the expression of the Fe-Sod to deal with excess Cu^+, soluble fractions from wild-type and *copA*$^-$ mutant grown in presence of excess $CuSO_4$ were analysed. *In-gel* SOD activity assay and Western blot analyses showed no differences in the

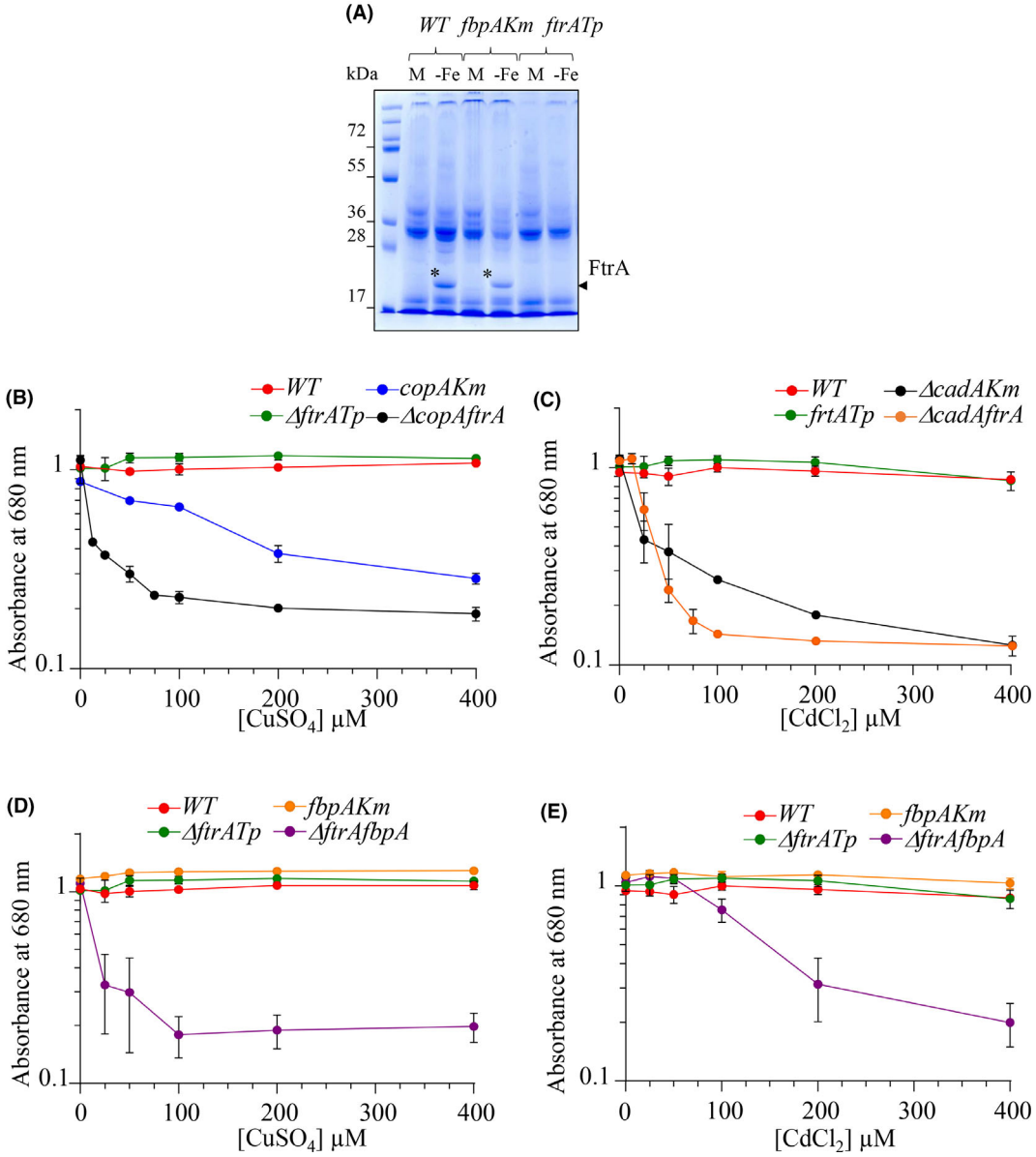

Fig. 5. Ftr iron import is also required for copper and cadmium tolerance when the efflux system is defective. SDS-PAGE showing the absence of FtrA (P19) in the periplasmic fraction of the corresponding mutant (A). Cells were grown in malate (M) or in iron-depleted malate medium (-Fe). FtrA is also involved in copper and cadmium tolerance. Growth inhibition of the Δ*copAftrA and* Δ*cadAftrA* in malate medium supplemented with increasing $CuSO_4$ (B) or $CdCl_2$ (C) concentrations under photosynthesis condition. Growth inhibition of the Δ*ftrAfbpA* in malate medium supplemented with increasing $CuSO_4$ (D) or $CdCl_2$ (E) concentrations under photosynthesis condition, in comparison with the wild-type and the single mutants. Cells were grown overnight for 18 h at 30°C under PS condition, before OD_{680nm} measurement. Results are the average of 3 independent experiments.

Fe-Sod activity in the wild-type samples in response to Cu^+ (Fig. 7A). On the contrary, in the *copA*$^-$ mutant, exposure to Cu^+ resulted in a ~ 2-fold increase of the SodB activity and amount in response to excess Cu^+. In *V. cholerae,* genes encoding the Mn-Sod (*vc2696* or *sodA*) and the Fe-Sod (*vc2045* or *sodB*) are found in the genome. However, *in-gel* SOD activity assay indicated that only SodB was active in our condition (Fig. 7B). As for the effect of copper in *R. gelatinosus*, both the activity and amount of SodB were induced (around 2- and 6-fold, respectively) in *V. cholerae copA*$^-$ cells, when challenged with $CuSO_4$ (Fig. 7B). The periplasmic copper protein CopI (Durand *et al*., 2015) is noteworthy induced under copper stress in *R. gelatinosus* and *V. cholerae* in response to Cu^+. Cadmium stress in *R. gelatinosus* and *V. cholerae* also resulted in the induction of SodB in the

CadA ATPase-deficient mutants (*accompanying paper* (Steunou *et al.*, 2020b)).

Together, both *R. gelatinosus* and *V. cholerae* showed induction of SodB under Cu^{+} stress. Importantly, SodB is the only functional SOD in these bacteria as *R. gelatinosus* lacks the Mn-Sod and Mn-Sod is not expressed or not functional in *V. cholerae* under our condition. Therefore, *R. gelatinosus* and *V. cholerae* can only express the Fe-Sod to deal with excess metal and superoxide.

We also analysed the SOD activity in response to excess $CuSO_4$ in *E. coli* for a set of Cu^{+} efflux mutants. As clearly shown in Figure 7C, addition of copper to the growth medium strongly induced the activity of the Mn-Sod in Δ*copA,* Δ*cusAcueO* and Δ*copAcusAcueO* mutants but not in the wild-type, demonstrating that accumulation of $CuSO_4$ induced the Mn-Sod. Concomitant to SodA induction, a drastic decrease in the Fe-Sod activity was observed. To further support these results, the expression level of the Mn-Sod was assessed on Western blots using the HisProbe that reacted with the 5 histidines in the N-ter of the *E. coli* Mn-Sod (Fig. 7C). The data confirmed the increased amount of Mn-Sod in the cytosolic fractions of the copper efflux-deficient mutants. Similar experiments were conducted using the ZntA mutant of *E. coli* to check the effect of Cd^{2+} on SOD activity. Likewise, excess Cd^{2+} in the medium resulted in an induced activity of the Mn-Sod and decreased activity of the Fe-Sod only in the ZntA mutant (*accompanying paper* (Steunou *et al.*, 2020b)). Altogether, these results showed that the accumulation of copper affected the expression and activity of superoxide dismutases presumably because of iron homoeostasis dysregulation linked to copper stress.

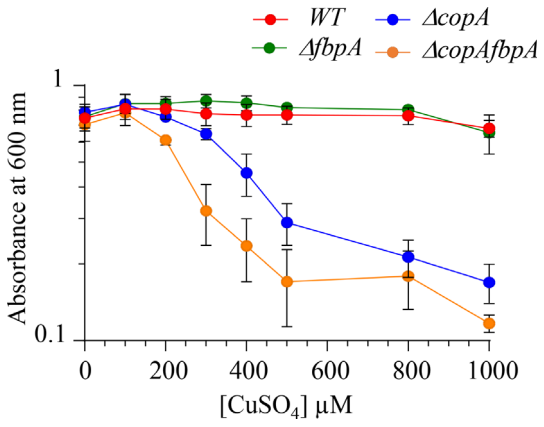

Fig. 6. FbpA is also involved in copper tolerance in *V. cholerae*. Growth inhibition of the Δ*copAfbpA* mutant in comparison with the *WT*, Δ*copA* and the Δ*fbpA* challenged with increasing $CuSO_4$ concentrations under aerobic condition. Cells were grown overnight for 16 h at 37°C before OD_{600nm} measurement. Results are the average of 3 independent experiments.

Discussion

The interplay between copper and iron dates back to the middle of the 19th century when copper was used as a therapeutic agent to treat anaemia. Copper was later shown to indirectly enhance haemoglobin formation by increasing iron absorption. This was brilliantly documented in the review by Paul Fox in 2003 (Fox, 2003). Another copper/iron interplay occurs in macrophages in the immune system. It was proposed that overloading the phagosome with toxic metal such as copper and limiting the availability of essential ions like iron are used to poison intracellular pathogens (Hood and Skaar, 2012; Neyrolles *et al.*, 2015). Several other indirect lines of evidence, mainly transcriptomics, support the involvement of iron in response to heavy metal excess (Gross *et al.*, 2000; Stadler and Schweyen, 2002; Teitzel *et al.*, 2006; Yoshihara *et al.*, 2006; Houot *et al.*, 2007; Chillappagari *et al.*, 2010); however, this has not been directly tested. In this study, using a random mutagenesis approach, we focused on metal excess-induced toxicity and response and demonstrated that iron transport/uptake plays a key role in Cu^{+} as well as Cd^{2+} excess-induced stress.

Previous studies in bacteria and eukaryotes showed that exposed [4Fe-4S] clusters are susceptible to damage by metals such as Cu^{+}, Ag^{+} and Cd^{2+} (Macomber and Imlay, 2009; Xu and Imlay, 2012; Vallieres *et al.*, 2017). It was suggested that this led to the accumulation of 'free iron' and potentially increased ROS stress *via* Fe-catalysed Fenton chemistry. However, beyond the generated oxidative stress that can be scavenged by the ROS detoxification system, this situation of [4Fe-4S] cluster degradation and loss of key metabolic enzymes will presumably force bacteria to react quickly and repair these clusters to survive. The nature of the iron source used to rebuild these [4Fe-4S] clusters is an opened question. Keyer and Imlay elegantly showed that upon exposure to peroxynitrite in *E. coli*, the [4Fe-4S] cluster of dehydratases was degraded and the 'released iron' originating from [4Fe-4S] degradation was rapidly sequestered and no more available for cellular processes (Keyer and Imlay, 1997). Therefore, for [4Fe-4S] cluster repair, most of the iron was imported from the external medium. Iron uptake is thus required to supply sufficient iron to the Fe-S machinery in response to peroxynitrite stress (Keyer and Imlay, 1997). Here, our study showed that similar events might take place in the case of Cu^{+} and Cd^{2+} stress, for which excess metal damage exposed [4Fe-4S], thus causing the release of iron. Paradoxically, despite the presence of Fe in the medium, cells might perceive the situation as an 'iron-starvation' situation and respond to it by inducing the expression of iron uptake systems to enhance Fe-import (Fig. 8). This raises the question of what happens to

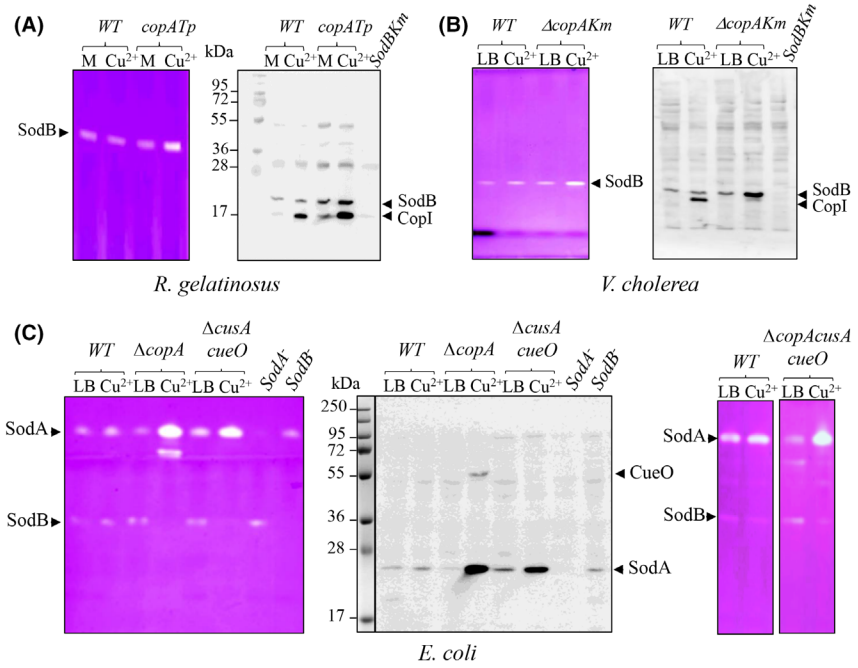

Fig. 7. Effect of excess copper on SOD activity. Induction of Fe-Sod activity and expression in response to excess $CuSO_4$ in *R. gelatinosus* wild-type and *copATp* mutant (A). Induction of Fe-Sod activity and expression in *V. cholerae* wild-type and Δ*copA* mutant (B). Induction of Mn-Sod activity and expression in the soluble fractions from the WT, Δ*copA,* Δ*cusAcueO and* Δ*copAcusAcueO* strains of *E. coli* (C). Proteins were labelled according to their size and expression profile. All cells were grown overnight in appropriate medium supplemented or not with 100 μM $CuSO_4$ (Cu^{2+}).

released iron. In addition to its possible sequestration by iron storage proteins, released iron could also be exported out of the cells by Fe^{2+}-efflux transporters to prevent iron overload and related damages. Our ICP-MS data did show a decrease in the amount of total iron content in *copATp* and Δ*cadATp* cells in agreement with a putative Fe^{2+}-efflux in these mutants, as in other species (Pi and Helmann, 2017). An additional stress imposed by Cu^{+} and Cd^{2+} excess was proposed to occur on the Fe-S cluster biogenesis (ISC) machinery. Indeed, Cu^{+} and Cd^{2+} appeared to directly bind and inhibit components of the *E. coli* ISC machinery (Chillappagari *et al.*, 2010; Tan *et al.*, 2014, 2017; Roy *et al.*, 2018). Inhibition of the ISC machinery will increase the demand for iron and would thus contribute to the activation of iron uptake systems.

In contrast to our results, Helbig *et al.* reported that iron uptake was downregulated when *E. coli* cells were exposed to Cd^{2+} (Helbig *et al.*, 2008). Nevertheless, these experiments were performed with strains with an affective Cd^{2+} efflux system (ZntA) that was able to expel Cd^{2+} from the cytoplasm and allow normal cellular growth. Indeed, a 10-min exposure to 100 μM $CdCl_2$ resulted in a significant induction of *zntA* expression (Helbig *et al.*, 2008). On the contrary, in a recent study, Xu *et al.* reported that Fe-uptake was required to maintain cell fitness during Zn^{2+} excess in *E. coli* and that excess Zn^{2+} led to a transient dysregulation of iron uptake (Xu *et al.*, 2019). They showed that iron uptake was upregulated by excess Zn^{2+} and once bacteria were adapted to excess Zn^{2+}, the system was switched off. Obviously, if the efflux system is efficient, it will provide sufficient protection against excess metal, as the need of upregulation of defence, iron uptake or Fe-S repair systems would no longer be justified or necessary to sustain growth. Thus, because the activity of the metal detoxification pumps can hide metal toxicity effects, mutants that lack the efflux pumps are suitable to test elevated metal stress and its consequences on iron homoeostasis. In *P. aeruginosa*, excess Cu^{+}, Zn^{2+}, Co^{2+}, Ni^{2+} or Cd^{2+} affects siderophore synthesis (Visca *et al.*, 1992; Teitzel *et al.*, 2006; Schalk *et al.*, 2020). It was shown that genes encoding synthesis of pyoverdine were upregulated in response to Cu^{+}, Zn^{2+} and Cd^{2+} suggesting that pyoverdine may protect the cells by sequestering heavy metals. Nevertheless, although able to chelate Cu^{+}, Zn^{2+} and Cd^{2+}, pyoverdine is highly iron specific and its affinity to iron is much more higher, indicating that it might rather provide the bacterium with iron under excess metal (Visca *et al.*, 1992; Teitzel *et al.*, 2006; Schalk *et al.*, 2020). In contrast, pyochelin has a broader specificity for cations and its synthesis was repressed by Cu^{+}, Cd^{2+}, Co^{2+} and Ni^{2+}. Inhibition of its synthesis under Cu^{+} excess would protect bacteria from Cu^{+}

poisoning (Teitzel *et al.*, 2006). In the oysters' pathogenic *Vibrio tasmaniensis LGP32* bacterium, comparative transcriptomic showed that the Cu^{+}-efflux ATPase CopA, as well as many iron (including FbpABC), siderophore uptake systems and Fe-S biogenesis genes were induced in the phagosomes (Vanhove *et al.*, 2016).

The mechanisms by which Cu^{+} or Cd^{2+} induces iron uptake are not yet well studied. Metals such as Co^{2+}, Zn^{2+} or Cu^{+} can displace or replace Fe^{2+} in the ferric uptake regulator Fur and may therefore affect Fur for DNA binding (Adrait *et al.*, 1999; Mills and Marletta, 2005; Vitale *et al.*, 2009). The facts that (i) induction of iron uptake system occurs with a variety of cations or superoxide generators that target [4Fe-4S], (ii) the demand for iron for the [4Fe-4S] regeneration is high and (iii) the observation that released iron is rapidly sequestered rather argue for a mechanism in which stressed cells respond to iron or Fe-S depletion. While the response seems to be Fur-independent for peroxynitrite stress (Keyer and Imlay, 1997), the involvement of regulatory factors, including Fur, remains to be investigated for the metallic stress.

Concomitant to the degradation of [4Fe-4S] clusters and iron homoeostasis dysregulation by excess Cu^{+} or Cd^{2+}, stressed cells also induce the expression of superoxide dismutases SodA or SodB. One may ask whether these enzymes are solely induced because of iron dysregulation or because they are required under Cu^{+} or Cd^{2+} stress. The induction of SODs is not fortuitous but functional. Indeed, mutants in which both the efflux system CopA or CadA and the superoxide dismutase SodB are missing are also extremely sensitive to Cu^{+} and to Cd^{2+} stress (*accompanying paper* (Steunou *et al.*, 2020b)).

The overall findings and the bacterial model depicted in Figure 8 to rationalize metal excess toxicity in bacteria could also apply to eukaryotes. It was recently shown that excess copper targets Fe-S clusters and ferredoxins in yeast (Vallieres *et al.*, 2017) and various studies reported that Cu^{+}, Cd^{2+}, Ni^{2+}, Cr^{3+} or Co^{2+} exposure in yeast (Stadler and Schweyen, 2002; Alkim *et al.*, 2013; Foster *et al.*, 2014; Johnson *et al.*, 2016), in plants (Yoshihara *et al.*, 2006) or in human (Fox, 2003; Davidson *et al.*, 2005) triggers iron deficiency responses and the induction of iron uptake systems. Together, these data point to the essential role of iron homoeostasis in response to excess heavy metal in eukaryotes as well, although other hypotheses including competition between metals and iron uptake may account for the iron deficiency status (Rubinelli *et al.*, 2002; Davidson *et al.*, 2005).

Extensive use of antibiotics in health care and agriculture has led to an increase in antibiotic resistance (Asante and Osei Sekyere, 2019). Metals that exhibit antimicrobial properties are used as alternatives to antibiotics in farming and agriculture. Nevertheless, the use of metals at high concentrations contributes to environment contamination and to co-selection of antibiotic resistance genes (Baker-Austin *et al.*, 2006; Purves *et al.*, 2018; Rensing *et al.*, 2018; Bischofberger *et al.*, 2020). The combination of excess Cu^{2+}, at very low concentration, and iron limitation poses a serious challenge to bacteria as shown in this work. This combination could be exploited in the course of metal-based

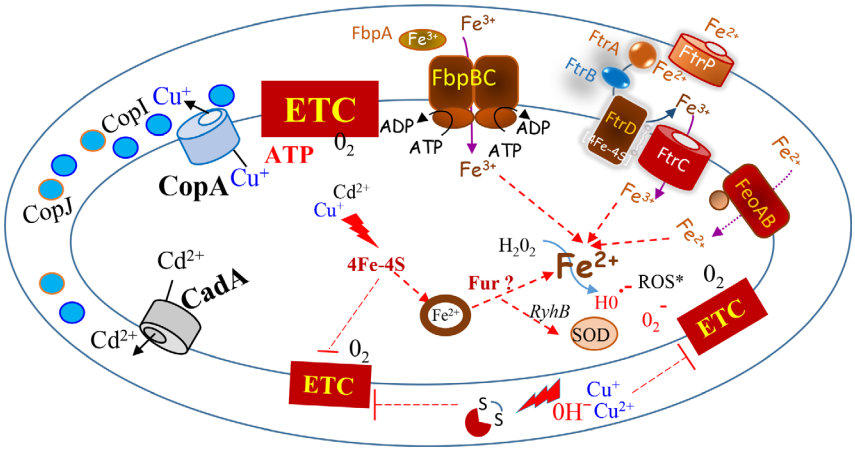

Fig. 8. Interplay between metal efflux, iron uptake and ROS detoxifying system. In the absence of the efflux ATPases CopA or CadA accumulation of Cu^{+} or Cd^{2+} in the cytosol led to the degradation of [4Fe-4S] clusters. 'Released iron' originating from this degradation could rapidly be sequestered or exported out of the cells, thus generating an iron-depleted status in the poisoned cells. Consequently, iron uptake is induced to rebuild [4Fe-4S] clusters and the superoxide dismutases are induced. It was supposed that released iron could generate ROS, but oxidative stress may be further exacerbated by the induction of Fe-uptake in response to damaged Fe-S clusters. ETC: electron transfer chains (respiration or photosynthesis) are also poisoned by excess metal. ETC generate ATP for the ATPases but can also generate superoxide.

antimicrobial treatments in agriculture, farming and drug design strategies.

Experimental procedures

Bacterial strains and growth

R. gelatinosus was grown at 30°C, in the dark aerobically (high oxygenation: 250 ml flasks containing 20 ml medium) or under light microaerobically (photosynthetic condition, in filled tubes with residual oxygen in the medium) in malate growth medium. *E. coli* and *V. cholerae* were grown overnight at 37°C in LB medium. Antibiotics (50 $\mu g\ ml^{-1}$), kanamycin (Km), spectinomycin (Sp), streptomycin (Sm) and trimethoprim (Tp), were added when appropriate.

Bacterial strains and plasmids are listed in Table S1. For growth inhibition under photosynthetic condition, strains were grown overnight in filled tubes and OD_{680nm} was measured. For *V. cholerae* OD_{600nm} was measured after overnight growth using the Tecan Infinite M200 luminometer (Tecan, Mannedorf, Switzerland).

Transposon mutagenesis and mutant selection

R. gelatinosus Δ*copRcadR* mutant was mutagenized using the EZ-Tn5-KAN-2-Tnp Transposome Kit (Epicentre) and following the manufacturer's protocol. Cells were transformed by electroporation (Steunou *et al*., 2013). Transformants were selected by plating cells onto malate plates containing Km, Tp and Sp. The colonies were first transferred on plates containing 50 μM of $CuSO_4$ to identify colonies sensitive to $CuSO_4$. Cu^+-sensitive clones were then screened for their Cd^{2+} sensitivity on 50 μM of $CdCl_2$. Among 4000 transformants screened, 10 clones were confirmed as sensitive to both Cu^+ and Cd^{2+}. Transposon insertion site of each clone was determined by sequencing the flanking region of the transposon.

Gene cloning, plasmid constructions and mutant strain construction

Standard methods were performed according to Sambrook *et al.* (1989) unless indicated otherwise. KS-fbpAKm was obtained from DNA isolated from Δ*copR-cadR-fbpA2::Tn5* digested by SgrAI and cloned into Bluescript KS+. This plasmid was used to inactivate *fbpA* by electroporation in the wild-type, *copATp*, Δ*cadATp* and Δ*ftrA*Tp mutants of *R.gelatinosus*. The *fbpBC* DNA fragment (2208 bp) was cloned into pGEM-T by PCR amplification using the primers fbpBC-For and fbpBC-Rev (Table S2). The resulting plasmid pGfbpBC was digested with Eco47III to delete 1088 fragment. The Tp cassette from p34S-Tp was inserted into the Eco47III site within *fbpBC* to create pGfbpBC::Tp. This plasmid was used to inactivate *fbpBC* in the wild-type, in *copAKm* and Δ*cadAKm* mutants of *R.gelatinosus*.

To inactivate *ftrA*, a 1 kb fragment was amplified using the primers ftrA-For and ftrA-Rev and cloned into the PCR cloning vector pGEM-T to give pGftrA. A 0.2-kb StuI and MscI fragment was deleted and replaced by the 0.7-kb Tp resistance cassette to disrupt the *ftrA* gene. The resulting recombinant plasmid was designated pGftrATp. This plasmid was used to inactivate *ftrA* by electroporation in the wild-type, in *copAKm*, Δ*cadAKm* and *fbpAKm* mutants in *R. gelatinosus*. Transformants were selected on malate plates supplemented with the appropriate antibiotics under aerobic condition. Genomic DNA was prepared from the ampicillin-sensitive transformants, and confirmation of the presence of the antibiotic resistance marker at the desired locus was performed by PCR. The pET28bFbpAH_6 plasmid was generated by cloning *fbpA* in the pET-28b plasmid. The *fbpA* gene was amplified by PCR from *R. gelatinosus* DNA using the fbpA-NcoI and fbpA-HindIII primers and cloned in pET-28b plasmid. The plasmid was integrated at the *fpbA* locus on the chromosome of *R. gelatinosus* by selecting for kanamycin resistance. The integration of this plasmid at the *fbpA* locus was confirmed by PCR on genomic DNA.

To construct Δ*copA* in *V. cholerae*, ~ 600 bp fragments upstream and downstream to the *copA (vc2215)* were amplified using primers oYo848 and oYo849, and oYo850 and oYo851 respectively. Resulting fragments were cloned into SmaI site of pCVD442 vector (Donnenberg and Kaper, 1991) using Gibson Assembly (Gibson *et al*., 2009), resulting in pEYY345. Similarly, to construct Δ*fbpA* in *V. cholerae,* ~ 600 bp fragments upstream and downstream to the *fbpA* (*vc0608*) were amplified using primers oYo854 and oYo855, and oYo856 and oYo857, respectively, and cloned into the pCVD442 vector, resulting in pEYY346. Subsequently, plasmid was transferred by conjugation to introduce mutation in *V. cholerae* by allelic exchange (Donnenberg and Kaper, 1991). DNA oligonucleotides used in this study are listed in Table S2.

SOD in-gel activity assay on non-denaturing gel electrophoresis

20 μg of soluble proteins was separated on a 10% non-denaturing polyacrylamide gel and stained for SOD activity as described in Weydert et al. (48), with minor modifications. Incubation with TEMED (0.85%) and Riboflavin-5-Phosphate (56 μM) was performed for 15 min at light and room temperature (RT), followed by the addition of nitroblue tetrazolium (2 $mg\ ml^{-1}$) and a 15 min incubation in the dark at RT. Gel was washed twice in ddH_2O and left in ddH_2O at RT on a light box until SOD-positive staining appeared.

Western blot and HisProbe-HRP detection

Equal amount of soluble proteins (20 μg) or periplasmic fractions was separated on SDS-PAGE and transferred onto a Hybond ECL Polyvinylidene difluoride membrane (GE Healthcare). Membrane was then probed with the HisProbe-HRP (horseradish peroxidase, from Pierce) according to the manufacturer's instruction. Positive bands were detected using a chemiluminescent HRP substrate according to the method of Haan and Behrmann (Haan and Behrmann, 2007). Image capture was performed with a ChemiDoc camera system (Bio-Rad).

Inductively coupled plasma mass spectrometry (ICP-MS) measurements

The concentrations of total iron in cells were measured by ICP-MS as described in Grassin-Delyle *et al.* (2019). Pellets of overnight grown cells in the presence or absence of 100 μM $CuSO_4$ or 100 μM $CdCl_2$ were washed with cold PBS buffer five times and stored at −80°C prior to ICP-MS analyses. Metal concentrations in the samples were calculated according to the standard curves. The values were normalized by the culture absorbance at 680 nm.

Periplasmic fraction preparation

R. gelatinosus cells were washed twice with 50 mM Tris-HCl (pH 7.8) and resuspended in the same buffer in the presence of 0.45 M sucrose, 1.3 mM EDTA and 0.6 mg ml^{-1} lysozyme. After 1h of incubation at 30°C with soft shaking, the extract was centrifuged for 15 min at 6000 r.p.m. The supernatant corresponds to the periplasmic fraction (Durand *et al.*, 2015).

mRNA preparation and RT-PCR

Total RNA was purified from wild-type cells grown in photosynthesis condition in malate medium (M), in an iron-depleted malate medium (-Fe) or in malate medium supplemented with 1 mM of $CuSO_4$ or 1 mM of $CdCl_2$ as described in (Steunou *et al.*, 2013). For semi-quantitative RT-PCR, cDNA was generated from 1 μg of total RNA with random hexamers using the Superscript IV (Invitrogen) and by following the manufacturer's protocol. PCR was done with 2 μl of cDNA with specific primers (Table S2) to amplify fragments of 16S, *pucA* (encoding the α subunit of LH2), *sodB* (encoding superoxide dismutase), *ftrA* and *fbpA* genes. Amplified products were analysed on a 1.4% agarose gel, and the bands were quantified using *imageJ* program. The relative amount was calculated based on the signal obtained in malate medium.

Acknowledgements

We gratefully acknowledge the support of the CNRS and the Microbiology Department of I2BC. We are very grateful to Prof. Dietrich H. Nies for providing *E. coli* strains. We also acknowledge the National BioResource Project, National Institute of Genetics, Japan. ICP-MS experiments were performed in the MasSpecLab facility in Versailles Saint-Quentin-en-Yvelines University.

Conflict of interest

The authors declare that they have no conflicts of interest with the contents of this manuscript.

Author contributions

AS.S., A.D., M.B., S.L. and S.O. designed research; AS.S., ML.B., M.B., Y.Y. and S.O. performed research; AS.S., A.D., M.B., S.L., ML.B. and S.O analysed data; AS.S., M.B. and S.O. wrote the paper.

References

Adrait, A., Jacquamet, L., Le Pape, L., Gonzalez de Peredo, A., Aberdam, D., Hazemann, J. L., *et al.* (1999) Spectroscopic and saturation magnetization properties of the manganese- and cobalt-substituted Fur (ferric uptake regulation) protein from *Escherichia coli*. *Biochemistry* **38:** 6248–6260.

Alkim, C., Benbadis, L., Yilmaz, U., Cakar, Z. P., and Francois, J. M. (2013) Mechanisms other than activation of the iron regulon account for the hyper-resistance to cobalt of a Saccharomyces cerevisiae strain obtained by evolutionary engineering. *Metallomics* **5:** 1043–1060.

Andreini, C., Banci, L., Bertini, I., and Rosato, A. (2008) Occurrence of copper proteins through the three domains of life: a bioinformatic approach. *J Proteome Res* **7:** 209–216.

Asante, J., and Osei Sekyere, J. (2019) Understanding antimicrobial discovery and resistance from a metagenomic and metatranscriptomic perspective: advances and applications. *Environ Microbiol Rep* **11:** 62–86.

Azzouzi, A., Steunou, A. S., Durand, A., Khalfaoui-Hassani, B., Bourbon, M. L., Astier, C., *et al.* (2013) Coproporphyrin III excretion identifies the anaerobic coproporphyrinogen III oxidase HemN as a copper target in the Cu^{+}-ATPase mutant *copA*$^{-}$ of *Rubrivivax gelatinosus*. *Mol Microbiol* **88:** 339–351.

Baker-Austin, C., Wright, M. S., Stepanauskas, R., and McArthur, J. V. (2006) Co-selection of antibiotic and metal resistance. *Trends Microbiol* **14:** 176–182.

Ballabio, C., Panagos, P., Lugato, E., Huang, J. H., Orgiazzi, A., Jones, A., *et al.* (2018) Copper distribution in European topsoils: An assessment based on LUCAS soil survey. *Sci Total Environ* **636:** 282–298.

Barwinska-Sendra, A., and Waldron, K. J. (2017) The role of intermetal competition and mis-metalation in metal toxicity. *Adv Microb Physiol* **70:** 315–379.

Bischofberger, A. M., Baumgartner, M., Pfrunder-Cardozo, K. R., Allen, R. C., and Hall, A. R. (2020) Associations between sensitivity to antibiotics, disinfectants and heavy metals in natural, clinical and laboratory isolates of *Escherichia coli*. *Environ Microbiol*. https://doi.org/10.1111/1462-2920.14986

Cao, J., Woodhall, M. R., Alvarez, J., Cartron, M. L., and Andrews, S. C. (2007) EfeUOB (YcdNOB) is a tripartite, acid-induced and CpxAR-regulated, low-pH Fe2+ transporter that is cryptic in Escherichia coli K-12 but functional in E. coli O157:H7. *Mol Microbiol* **65:** 857–875.

Carlioz, A., and Touati, D. (1986) Isolation of superoxide dismutase mutants in *Escherichia coli*: is superoxide dismutase necessary for aerobic life? *EMBO J* **5:** 623–630.

Chillappagari, S., Seubert, A., Trip, H., Kuipers, O. P., Marahiel, M. A., and Miethke, M. (2010) Copper stress affects iron homeostasis by destabilizing iron-sulfur cluster formation in *Bacillus subtilis*. *J Bacteriol* **192:** 2512–2524.

Davidson, T., Chen, H., Garrick, M. D., D'Angelo, G., and Costa, M. (2005) Soluble nickel interferes with cellular iron homeostasis. *Mol Cell Biochem* **279:** 157–162.

Djoko, K. Y., and McEwan, A. G. (2013) Antimicrobial action of copper is amplified via inhibition of heme biosynthesis. *ACS Chem Biol* **8:** 2217–2223.

Donnenberg, M. S., and Kaper, J. B. (1991) Construction of an eae deletion mutant of enteropathogenic *Escherichia coli* by using a positive-selection suicide vector. *Infect Immun* **59:** 4310–4317.

Durand, A., Azzouzi, A., Bourbon, M. L., Steunou, A. S., Liotenberg, S., Maeshima, A., *et al*. (2015) c-type cytochrome assembly is a key target of copper toxicity within the bacterial periplasm. *MBio* **6:** e01007-15.

Fantino, J. R., Py, B., Fontecave, M., and Barras, F. (2010) A genetic analysis of the response of *Escherichia coli* to cobalt stress. *Environ Microbiol* **12:** 2846–2857.

Foster, A. W., Dainty, S. J., Patterson, C. J., Pohl, E., Blackburn, H., Wilson, C., *et al*. (2014) A chemical potentiator of copper-accumulation used to investigate the iron-regulons of Saccharomyces cerevisiae. *Mol Microbiol* **93:** 317–330.

Fox, P. L. (2003) The copper-iron chronicles: the story of an intimate relationship. *Biometals* **16:** 9–40.

Gibson, D. G., Young, L., Chuang, R. Y., Venter, J. C., Hutchison, C. A. 3rd, and Smith, H. O. (2009) Enzymatic assembly of DNA molecules up to several hundred kilobases. *Nat Methods* **6:** 343–345.

Grassin-Delyle, S., Martin, M., Hamzaoui, O., Lamy, E., Jayle, C., Sage, E., *et al*. (2019) A high-resolution ICP-MS method for the determination of 38 inorganic elements in human whole blood, urine, hair and tissues after microwave digestion. *Talanta* **199:** 228–237.

Gross, C., Kelleher, M., Iyer, V. R., Brown, P. O., and Winge, D. R. (2000) Identification of the copper regulon in Saccharomyces cerevisiae by DNA microarrays. *The Journal of biological chemistry* **275:** 32310–32316.

Gunther, M. R., Hanna, P. M., Mason, R. P., and Cohen, M. S. (1995) Hydroxyl radical formation from cuprous ion and hydrogen peroxide: a spin-trapping study. *Arch Biochem Biophys* **316:** 515–522.

Haan, C., and Behrmann, I. (2007) A cost effective non-commercial ECL-solution for Western blot detections yielding strong signals and low background. *J Immunol Methods* **318:** 11–19.

Helbig, K., Grosse, C., and Nies, D. H. (2008) Cadmium toxicity in glutathione mutants of *Escherichia coli*. *J Bacteriol* **190:** 5439–5454.

Hood, M. I., and Skaar, E. P. (2012) Nutritional immunity: transition metals at the pathogen-host interface. *Nat Rev Microbiol* **10:** 525–537.

Houot, L., Floutier, M., Marteyn, B., Michaut, M., Picciocchi, A., Legrain, P., *et al*. (2007) Cadmium triggers an integrated reprogramming of the metabolism of Synechocystis PCC6803, under the control of the Slr1738 regulator. *BMC Genom* **8:** 350.

Imlay, J. A. (2019) Where in the world do bacteria experience oxidative stress? *Environ Microbiol* **21:** 521–530.

Johnson, A. J., Veljanoski, F., O'Doherty, P. J., Zaman, M. S., Petersingham, G., Bailey, T. D., *et al*. (2016) Revelation of molecular basis for chromium toxicity by phenotypes of Saccharomyces cerevisiae gene deletion mutants. *Metallomics* **8:** 542–550.

Kershaw, C. J., Brown, N. L., Constantinidou, C., Patel, M. D., and Hobman, J. L. (2005) The expression profile of Escherichia coli K-12 in response to minimal, optimal and excess copper concentrations. *Microbiology* **151:** 1187–1198.

Keyer, K., and Imlay, J. A. (1997) Inactivation of dehydratase [4Fe-4S] clusters and disruption of iron homeostasis upon cell exposure to peroxynitrite. *J Biol Chem* **272:** 27652–27659.

Krumschnabel, G., Manzl, C., Berger, C., and Hofer, B. (2005) Oxidative stress, mitochondrial permeability transition, and cell death in Cu-exposed trout hepatocytes. *Toxicol Appl Pharmacol* **209:** 62–73.

Liu, M. M., Boinett, C. J., Chan, A. C. K., Parkhill, J., Murphy, M. E. P., and Gaynor, E. C. (2018) Investigating the *Campylobacter jejuni* transcriptional response to host intestinal extracts reveals the involvement of a widely conserved iron uptake system. *MBio* **9:** 1–18.

Macomber, L., and Hausinger, R. P. (2011) Mechanisms of nickel toxicity in microorganisms. *Metallomics* **3:** 1153–1162.

Macomber, L., and Imlay, J. A. (2009) The iron-sulfur clusters of dehydratases are primary intracellular targets of copper toxicity. *Proc Natl Acad Sci USA* **106:** 8344–8349.

Masse, E., and Gottesman, S. (2002) A small RNA regulates the expression of genes involved in iron metabolism in *Escherichia coli*. *Proc Natl Acad Sci USA* **99:** 4620–4625.

Mills, S. A., and Marletta, M. A. (2005) Metal binding characteristics and role of iron oxidation in the ferric uptake regulator from *Escherichia coli*. *Biochemistry* **44:** 13553–13559.

Neyrolles, O., Wolschendorf, F., Mitra, A., and Niederweis, M. (2015) Mycobacteria, metals, and the macrophage. *Immunol Rev* **264:** 249–263.

Nunes, I., Jacquiod, S., Brejnrod, A., Holm, P. E., Johansen, A., Brandt, K. K., *et al.* (2016) Coping with copper: legacy effect of copper on potential activity of soil bacteria following a century of exposure. *FEMS Microbiol Ecol* **92:** fiw175.

Parker Siburt, C. J., Mietzner, T. A., and Crumbliss, A. L. (2012) FbpA–a bacterial transferrin with more to offer. *Biochim Biophys Acta* **1820:** 379–392.

Payne, S. M., Mey, A. R., and Wyckoff, E. E. (2016) Vibrio iron transport: evolutionary adaptation to life in multiple environments. *Microbiol Mol Biol Rev* **80:** 69–90.

Pi, H., and Helmann, J. D. (2017) Ferrous iron efflux systems in bacteria. *Metallomics* **9:** 840–851.

Purves, J., Thomas, J., Riboldi, G. P., Zapotoczna, M., Tarrant, E., Andrew, P. W., *et al*. (2018) A horizontally gene transferred copper resistance locus confers hyper-resistance to antibacterial copper toxicity and enables survival of community acquired methicillin resistant *Staphylococcus aureus* USA300 in macrophages. *Environ Microbiol* **20:** 1576–1589.

Rensing, C., Moodley, A., Cavaco, L. M., and McDevitt, S. F. (2018) Resistance to metals used in agricultural production. *Microbiol Spectr* **6:** 1–24.

Roy, P., Bauman, M. A., Almutairi, H. H., Jayawardhana, W. G., Johnson, N. M., and Torelli, A. T. (2018) Comparison of the response of bacterial IscU and SufU to Zn(2+) and select transition-metal ions. *ACS Chem Biol* **13:** 591–599.

Rubinelli, P., Siripornadulsil, S., Gao-Rubinelli, F., and Sayre, R. T. (2002) Cadmium- and iron-stress-inducible gene expression in the green alga *Chlamydomonas reinhardtii*: evidence for H43 protein function in iron assimilation. *Planta* **215:** 1–13.

Sambrook, J., Fritsch, E. F., and Maniatis, T. (1989) *Molecular Cloning, A Laboratory Manual*, 2nd edn. New York, NY: Cold Spring Harbor.

Schalk, I. J., Rigouin, C., and Godet, J. (2020) An overview of siderophore biosynthesis among fluorescent Pseudomonads and new insights into their complex cellular organization. *Environ Microbiol* **22:** 1447–1466.

Stadler, J. A., and Schweyen, R. J. (2002) The yeast iron regulon is induced upon cobalt stress and crucial for cobalt tolerance. *The Journal of biological chemistry* **277:** 39649–39654.

Steunou, A. S., Liotenberg, S., Soler, M. N., Briandet, R., Barbe, V., Astier, C., and Ouchane, S. (2013) EmbRS a new two-component system that inhibits biofilm formation and saves Rubrivivax gelatinosus from sinking. *Microbiologyopen* **2:** 431–446.

Steunou, A. S., Durand, A., Bourbon, M. L., Babot, M., Liotenberg, S., and Ouchane, S. (2020a) Cadmium and Copper Cross-tolerance. Cu^{+} alleviates Cd^{2+} toxicity, and both cations target the porphyrin biosynthesis pathway in *Rubrivivax gelatinosus*. *Front Microbiol* (In press) https://doi.org/10.3389/fmicb.2020.00893

Steunou, A. S., Babot, M., Bourbon, M. L., Tambosi, R., Durand, A., Liotenberg, S., *et al*. (2020b) Additive effects of metal excess and superoxide, a highly toxic mixture in bacteria. *Microb Biotechnol* (In press) https://doi.org/10.1111/1751-7915.13589

Tan, G., Cheng, Z., Pang, Y., Landry, A. P., Li, J., Lu, J., and Ding, H. (2014) Copper binding in IscA inhibits iron-sulphur cluster assembly in *Escherichia coli*. *Mol Microbiol* **93:** 629–644.

Tan, G., Yang, J., Li, T., Zhao, J., Sun, S., Li, X., *et al.* (2017) Anaerobic copper toxicity and iron-sulfur cluster biogenesis in *Escherichia coli*. *Appl Environ Microbiol* **83:** 1–11.

Teitzel, G. M., Geddie, A., De Long, S. K., Kirisits, M. J., Whiteley, M., and Parsek, M. R. (2006) Survival and growth in the presence of elevated copper: transcriptional profiling of copper-stressed Pseudomonas aeruginosa. *J Bacteriol* **188:** 7242–7256.

Troxell, B., and Hassan, H. M. (2013) Transcriptional regulation by Ferric Uptake Regulator (Fur) in pathogenic bacteria. *Front Cell Infect Microbiol* **3:** 59.

Turner, R. J. (2017) Metal-based antimicrobial strategies. *Microbial Biotechnol* **10:** 1062–1065.

Vallieres, C., Holland, S. L., and Avery, S. V. (2017) Mitochondrial ferredoxin determines vulnerability of cells to copper excess. *Cell Chem Biol* **24:** 1228–1237.e3.

Vanhove, A. S., Rubio, T. P., Nguyen, A. N., Lemire, A., Roche, D., Nicod, J., *et al*. (2016) Copper homeostasis at the host vibrio interface: lessons from intracellular vibrio transcriptomics. *Environ Microbiol* **18:** 875–888.

Visca, P., Colotti, G., Serino, L., Verzili, D., Orsi, N., and Chiancone, E. (1992) Metal regulation of siderophore synthesis in Pseudomonas aeruginosa and functional effects of siderophore-metal complexes. *Appl Environ Microbiol* **58:** 2886–2893.

Vitale, S., Fauquant, C., Lascoux, D., Schauer, K., Saint-Pierre, C., and Michaud-Soret, I. (2009) A ZnS(4) structural zinc site in the Helicobacter pylori ferric uptake regulator. *Biochemistry* **48:** 5582–5591.

Xu, F. F., and Imlay, J. A. (2012) Silver(I), mercury(II), cadmium(II), and zinc(II) target exposed enzymic iron-sulfur clusters when they toxify *Escherichia coli*. *Appl Environ Microbiol* **78:** 3614–3621.

Xu, Z., Wang, P., Wang, H., Yu, Z. H., Au-Yeung, H. Y., Hirayama, T., *et al*. (2019) Zinc excess increases cellular demand for iron and decreases tolerance to copper in *Escherichia coli*. *J Biol Chem* **294:** 16978–16991.

Yoshihara, T., Hodoshima, H., Miyano, Y., Shoji, K., Shimada, H., and Goto, F. (2006) Cadmium inducible Fe deficiency responses observed from macro and molecular views in tobacco plants. *Plant Cell Rep* **25:** 365–373.

Supporting information

Additional supporting information may be found online in the Supporting Information section at the end of the article.

Table S1. Bacterial strains and plasmids used in this work.

Table S2. DNA oligonucleotides used in this work.

Fig. S1. Tn mapping within *fbpA* and phenotype of the selected *fbpA*::Tn mutants. A. Tn mutagenesis mapping. Position of Tn within *fbpA* gene are indicated. B. Growth of Δ*copRcadR* (**1**) and ΔcopRcadR-fbpA::Tn5 mutants (**2-6**) on agar plates in malate medium (M) or malate supplemented with $CuSO_4$ or $CdCl_2$.

Fig. S2. A. Organization of the gene clusters and iron transport systems involved in iron acquisition in *R. gelatinosus.* Fur box sequences within the promoters of the identified clusters are shown. Fur boxes from *fecI* and *fhuA* iron regulated genes were used in the alignement. B. *R. gelatinosus* iron transport systems. FbpABC and FtrAPBCD are the major inner membrane iron transporters identified in this

study. Genes encoding other systems including TonB-dependent receptor family and siderophores importers (Fec, Fhu, Fpv...) are also present in the bacterium genome.

Fig. S3. Expression profiles (semi-quantitative RT-PCR) of *fbpA* and *ftrA* genes under various metal stress condition. A. Expression profiles (semi-quantitative RT-PCR) of *fbpA*, *ftrA* genes in *WT* cells grown under photosynthesis in Malate (M) medium, iron depleted Malate medium (-Fe), or Malate medium supplemented with 1 mM $CuSO_4$ or $CdCl_2$. The *pucA* gene encoding the light harvesting II α-subunit, *sodB* encoding the superoxide dismutase, and the 16S Rrna were used as references to normalize the relative expression of the induced genes. B. The results are expressed as fold changes of the expression of target genes in modified malate medium ($-$Fe, $+Cu^{+}$, $+Cd^{2+}$) relative to their expression in malate medium (M).

